THE EVOLUTION OF CRANIAL MODULARITY AND INTEGRATION IN THE

CAVIOMORPHA LINEAGE (MAMMALIA, RODENTIA)

by

GENEVIEVE VIOLET PERDUE

A THESIS

Presented to the Department of Earth Sciences
and the Graduate School of the University of Oregon
in partial fulfillment of the requirements
for the degree of
Master of Science

September 2017

THESIS APPROVAL PAGE

Student: Genevieve Violet Perdue

Title: The Evolution of Cranial Modularity and Integration in the Caviomorpha Lineage (Mammalia, Rodentia)

This thesis has been accepted and approved in partial fulfillment of the requirements for the Master of Science degree in the Department of Earth Sciences by:

Samantha S.B. Hopkins	Chairperson
Edward B. Davis	Member
Stephen R. Frost	Member
David A. Sutherland	Member

and

Sara D. Hodges	Interim Vice Provost and Dean of the Graduate School

Original approval signatures are on file with the University of Oregon Graduate School.

Degree awarded September 2017

THESIS ABSTRACT

Genevieve Violet Perdue

Master of Science

Department of Earth Sciences

September 2017

Title: The Evolution of Cranial Modularity and Integration in the Caviomorpha Lineage (Mammalia, Rodentia)

Caviomorph rodents arrived from Africa as sweepstakes colonists to the South American island continent between 54 and 37 Ma, and subsequently underwent a rapid and widespread adaptive radiation beginning in the middle Eocene. The geographic isolation of South America gave rise to a number of endemic mammal species that filled a wide variety of ecological niches. The resulting size of caviomorph rodents spanned over three orders of magnitude, making them an intriguing lineage to explore the morphological and ecological implications of size evolution. Here, I explore the morphological cranial patterns of extinct and extant caviomorph taxa using 2D landmark-based geometric morphometric analysis. Results are key to advancing our understanding of the effects phylogeny and body size have on cranial morphology of caviomorphs (and more broadly, mammals). This study indicates a deviation from the mammalian modular patterns determined a priori, suggesting unique evolutionary processes at play during the caviomorph adaptive radiation.

CURRICULUM VITAE

NAME OF AUTHOR: Genevieve Violet Perdue

GRADUATE AND UNDERGRADUATE SCHOOLS ATTENDED:

     University of Oregon, Eugene
     University of California, Davis
     Santa Rosa Junior College, Santa Rosa

DEGREES AWARDED:

     Master of Science, Vertebrate Paleontology, 2017, University of Oregon
     Bachelor of Science, Evolution Ecology and Biodiversity, 2013, University of California,
         Davis
     Transfer, Biochemistry, 2011, Santa Rosa Junior College

AREAS OF SPECIAL INTEREST:

     Morphological Evolution
     Paleoecology

PROFESSIONAL EXPERIENCE:

     Graduate Employee, University of Oregon, August 2015-September 2017

     Field Manager, Sonoma County Conservation Action, February 2014-August 2015

     Research Assistant, University of California, Davis, September 2012-August 2015

GRANTS, AWARDS, AND HONORS:

     Baldwin Travel Scholarship, Master's Thesis, University of Oregon, 2016

     Phi Sigma Biological Sciences Honor Society, UC Davis Chapter, 2013

ACKNOWLEDGMENTS

TABLE OF CONTENTS

LIST OF FIGURES

LIST OF TABLES

CHAPTER I

INTRODUCTION

Caviomorph rodents evolved from African hystricognaths before migrating from South Africa to South America approximately 54-37Ma (Hussain et al. 1978, Flynn and Wyss 1988). Currently, the scientific consensus postulates that caviomorph sweepstakes colonist ancestors rafted across the Atlantic Ocean, which was at least a 1,000km distance at the time (Lavocat 1969, Martin 1994, Huchon and Douzery 2001). The odds of successful colonization may have been enhanced by the presence of "stepping stone" islands between Africa and South America, favorable paleocurrents and paleowinds, a cooling climate, and changing oceanographic currents caused by the opening of Southern Ocean gateways and decreasing solar insolation at the Eocene-Oligocene boundary (Wyss et al. 1993, Flynn and Wyss 1998, Houle 1999, Huchon and Douzery 2001, Liu et al. 2009). Upon arrival, the lineage experienced an extensive adaptive radiation on the South American continent, which was geographically isolated from approximately 65-80Ma (Flynn and Wyss 1998) until 3Ma (Poux et al. 2006).

Members of Caviomorpha radiated from a small number of original sweepstakes colonists to produce morphologically diverse descendants (Vassallo and Verzi 2001, Weisbecker and Schmid 2007, Alvarez et al. 2015).This adaptive radiation resulted in diverse lineage ecologies including semi-aquatic, fossorial, subterranean, arboreal and epigean, as well as the associated occupancy of a wide variety of habitats (Mares and Ojeda 1982, Nowak 1991, Eisenberg and Redford 1999, Elissamburu and Vizcaino 2004, Morgan 2009, Alvarez et al. 2015, Patton et al. 2015) Today, extant caviomorph body masses span over three orders of magnitude, from 3.7kg to 81kg (Millien 2008), whereas extinct species masses reached at least 350kg (Millien 2008, Rindernknecht and Blanco 2008, Millien and Bovy 2010). As descendants of Old World hystricomorph rodents, caviomorph crania are

structurally unique relative to other groups of rodents, in possessing a cranial morphology known as the hystricomorph condition (Hautier et al. 2007), in which the medial masseter muscle passes through an enlarged infraorbital foramen between the attachments to the zygomatic arch and the rostrum (Figure 1). This morphology is an adaptation within the primarily herbivorous hystricognath lineage, with the masseter muscle proportions enabling stronger bite force of the back molars, and adding increased stress to the orbital region the closer the bite point is to the temporomandibular joint (Cox et al. 2012, Maestri et al. 2016). The considerable temporal depth, ecomorphological breadth, and long-term geographic isolation enabling the South American Caviomorpha radiation makes this lineage an excellent model with which to explore patterns of evolutionary change in morphology (Álvarez et al. 2015).
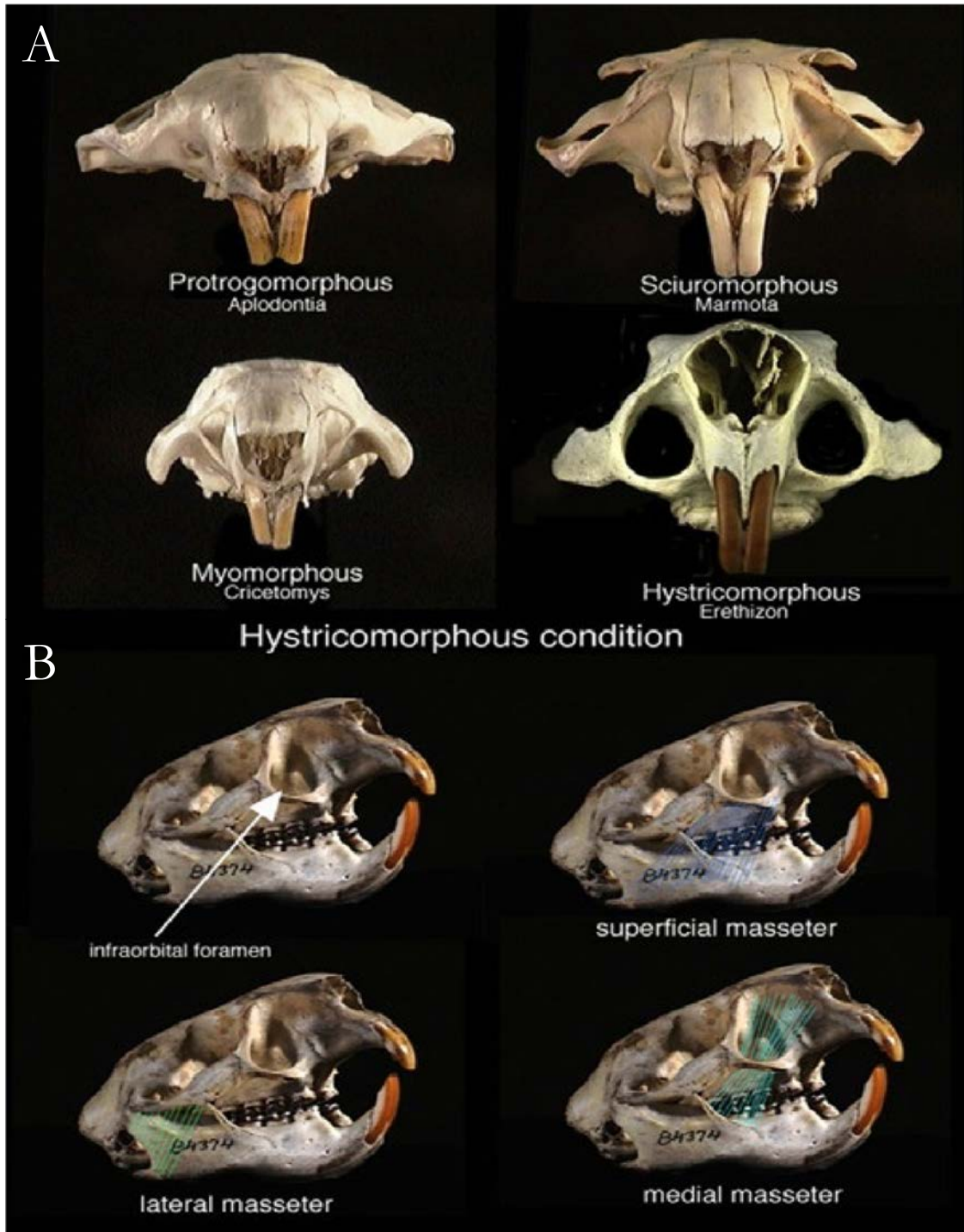
Figure 1. Hystricomorphous condition of rodent crania (A) morphology of protrogomorphous, sciuromorphous, myomorphous, hystricomorphous conditions, (B) hystricomorphous condition masseter alignment. Modified from Animaldiversity.org.

Mammalian skull morphology is a product of the evolutionary, functional, structural, and developmental forces exerted upon it (Zelditch et al. 2012). Traits linked by evolutionary history, spatial proximity, or developmental pathways are key components influencing morphological evolution (Olson and Miller in 1958, Vermeij 1973, Emerson and Hastings 1998, Bolker 2000, Pigliucci and Preston 2004). In 1958, Olson and Miller postulated that such linked traits could be integrated such that they would influence each other more than unlinked traits, forming groups of autonomous or semi-autonomous clusters known as modules (Goswami 2006). The joint processes of modularity and integration have an important impact on the directions of evolutionary change because they influence a structure's evolutionary ability to respond to selection pressures (Ackermann & Cheverud 2004, Marroig et al. 2009, Goswami et al. 2014). More specifically, integration is described as the tendency of specific traits to vary in a coordinated manner between individuals, and modularity as the concentration of integrated points within specific regions (Klingenberg 2013). Such trait associations have the potential to either foster the coordinated evolution of linked traits or to limit trait variation along different morphospace dimensions (Goswami 2006, Porto et al. 2009). The relatively independent nature of modules offers a novel method for exploring entire networks of traits in contrast with studying one trait at a time (Goswami 2006).

Currently, few studies empirically explore modularity more broadly than at the genus or species level, so more data are needed, particularly at higher taxonomic levels, to determine large scale patterns and significance of modularity (Marroig et al. 2009, Goswami and Polly 2010). In addition to providing new data for the exploration of mammalian modularity, studying caviomorph modularity is a useful tool for deciphering morphological patterns present throughout their ecologically unique South American island adaptive radiation.

Modularity is hypothesized to have the potential to both inhibit the rate of evolution by limiting the possible trait variations that can be selected from in linked traits (the constraint hypothesis), and accelerate the rate of evolution in cases where morphologically disparate or autonomous modules are selected for (the facilitation hypothesis) (Goswami and Polly 2010). Furthermore, modules themselves can also evolve, resulting in traits becoming more or less linked with time, further complicating studies. Existing modular studies of mammal crania consistently yield six significant modules: the anterior-oral-nasal (AON), molar (MR), orbit (ORB), zygomatic-pterygoid (ZP), condyle-basal (CB) and cranial vault (CV) groups (Goswami 2006, Goswami and Polly 2010). Additionally, Goswami and Polly's (2010) analysis on carnivorans and primates revealed that there is no simple pattern of the constraint or facilitation hypotheses present, but rather some evidence in support of constraint (eight of 24 analyses) and some data failing to support either (14 of 24 analyses). The explanation provided for these patterns is that either (1) constraint and facilitation could be co-occurring and counteracting each other, or that (2) there is not a strong correlation between integration and morphological evolution (Goswami and Polly 2010). To further understand the relationship between morphological change and modular integration in mammals, it must be explored in additional mammalian taxa. For caviomorph rodents, I have assessed how modularity and integration relate to changes in body mass, one axis of morphological disparity, as well as explored the phylogenetic effects of modular change within the lineage. This information will provide important insight into the modular patterns associated with the caviomorph lineage; a lineage with a unique cranial morphology that underwent a widespread adaptive radiation.

Shape analysis is a critical component of identifying the many possible forces at play in the determination of morphological diversity. Over the past two decades, morphometrics has become a leading analytical technique for quantifying shape variables and patterns within biological systems (Rohlf 1990, Rohlf and Marcus 1993, Adams et al. 2004 & 2013, Webster and Sheets 2010, Zelditch

et al. 2012, Cardini 2016). This method enables rigorous statistical shape analysis on physical measurements for comparative morphology, and is a useful tool for communicating such results with numerically driven visualizations (Webster and Sheets 2010, Zelditch et al. 2012). This study utilizes landmark-based geometric morphometrics, which is a method of shape summarization from data collected at landmarks, which are discrete anatomical points represented by Cartesian coordinates (Webster and Sheets 2010, Zelditch et al. 2012).

This study seeks to answer two questions. The first question that must be addressed is: what are the cranial modules in caviomorph modules? The answer to this question can then be applied to the second question: do changes in cranial modularity and integration contribute to the morphological diversity and variation we see in the caviomorph lineage? Combined, the answers to these questions will provide insight into which traits are correlated and which are autonomous, as well as the patterns associated with shifting morphological traits through time.

My thesis explores the impacts of a broad adaptive radiation and a unique zygomasseteric system on the modularity and integration of caviomorph rodent skulls over the past 30 million years. The passage of the medial masseter through an enlarged infraorbital foramen, the increased molar bite force relative to other rodents, and the resulting increased strain on the orbital region may correspond to unique morphological patterns. Consequently, it is first necessary to establish module identities rather than using *a priori* definitions (Goswami 2006, Goswami and Polly 2010).

Hypotheses

I: The unique hystricomorphous cranial morphology and broad adaptive radiation of caviomorph rodents will result in modules that deviate from the anterior oral-nasal, molar, basicranial, orbit, zygomatic-pterygoidm and vault mammalian modules that have been previously described. The

modified path of the medial masseter, along with the associated changes to the infraorbital foramen, molar bite force, and pressure exerted on the orbit will be reflected by a unique association of traits to this group.

II: Caviomorph species with deeper divergences will have less integrated cranial modules, suggesting less specialized morphologies, and species with shallower divergences will have more integrated modules, indicating specialized morphologies. Additionally, as body size increases, cranial module integration will increase as a result of morphological constraint, as niche space becomes limited to more fossorial and semiaquatic forms. Throughout the adaptive radiation, increasing competition and decreasing available niche space will dictate more integrated structures that have less variation to select for.

CHAPTER II

MATERIALS AND METHODS

Extant specimen photographs were collected at the American Museum of Natural History (AMNH), the Museum of Vertebrate Zoology (MVZ) and the Field Museum of Natural History (FMNH), and fossil specimen photographs were collected from FMNH. All specimen photographs included a scale bar, and were captured with a mounted Canon Rebel DSLR with the exception of *Josephoartigasia monesi*, which was landmarked from published images in Rinderknecht and Blanco's 2008 descriptive paper. Three to five individuals per extant species were collected, with male and female representatives to account for sexual dimorphism. For each fossil species, one individual of undetermined sex was collected. In total, 32 Caviomorph species of varying ecologies are represented in this study: 30 extant species, and two extinct species (Table 1).

Table 1. Families, genera, species and ecologies included in analysis. Ecological information from Animaldiversity.org, IUCNredlist.org.

Family	Species	# specimens	Ecology
Bathyergidae	*Cryptomys hottentotus*	5	fossorial
Caviidae	*Cavia porcellus*	5	epigean
	Cavia tschudii	5	epigean
	Dolichotis patagonum	4	fossorial
	Hydrochoerus hydrochaeris	5	semiaquatic
	Microcavia niata	5	fossorial
Chinchillidae	*Chinchilla lanigera*	5	epigean
	Lagidium peruanum	5	epigean
	Lagidium viscacia	5	epigean
	Lagostomus maximus	5	fossorial
Ctenomyidae	*Ctenomys colburni*	4	subterranean
	Ctenomys dorsalis	5	subterranean
	Ctenomys fulvus	5	subterranean
	Ctenomys mendocinus	5	fossorial
Dasyproctidae	*Dasyprocta fuliginosa*	1	epigean/cursorial
	Dasyprocta punctada	5	epigean
	Neoreomys australis(†)	1	Epigean/cursorial
Dinomyidae	*Dinomys branickii*	4	fossorial
	Josephoartigasia monesi(†)	1	semiaquatic

Erethizontidae	*Coendou mexicanus*	5	arboreal
	Erethizon dorsatum	5	epigean/sometimes arboreal
Echimyidae	*Mesomys hispidus*	5	arboreal
	Proechimys brevicauda	3	epigean
	Proechimys cuvieri	5	epigean
	Proechimys semispinosus	5	epigean
	Proechimys simonsi	4	epigean
	Proechimys steerei	4	epigean
	Thricomys apereoides	2	epigean
Octodontidae	*Aconaemys sagei*	5	subterranean
	Octodon degus	5	semi-fossorial
	Spalacopus cyanus	5	subterranean

Sixteen dorsal landmarks were chosen from Álvarez et al.'s 2013 Caviomorph geometric morphometric study to represent cranial shape. Two-dimensional landmarks were implemented on the midline and right side of each dorsal photograph using **TpsDig2** (Rohlf 2010) (Table 2, Figure 2). Figures were reflected prior to landmarking in cases where the left side of the skull was more intact than the right.

Table 2. Description of cranial dorsal landmarks modified from Álvarez et al. (2013).

Landmark #	Definition
1	Anterior lower end of premaxilla bone
2	Anterior end of nasal bone
3	Posterior end of nasal bone suture
4	Suture between premaxilla, nasal and frontal bones
5	Suture between premaxilla, maxilla and frontal bones
6	Posterior tip of zygomatic arch
7	Dorsal meeting of jugal and squamosal bones
8	Meeting of maxillary and lacrimal bones on anterior margin of orbit
9	Meeting of lacrimal and frontal bones on anterior margin of orbit
10	Suture between maxilla, lacrimal and frontal bones
11	Most dorsal point of external auditory meatus
12	Suture between squamosal, occipital and tympanic bones
13	Suture between squamosal, frontal and occipital bones
14	Suture between squamosal, frontal and parietal bones
15	Midline meeting of frontal and parietal bones
16	Most posterior point of skull

Figure 2. Distribution of dorsal cranial landmarks #1-16.

Each individual landmarked specimen was saved to a **.tps** file before being imported into R (R Core Team, 2015). Species landmark means were calculated and then aligned with Generalized Procrustes Analysis using the **geomorph** package (Adams and Otarola-Castillo 2013, Adams et al. 2014) to isolate allometric affects while eliminating scale as a factor.

Following the methods detailed in Goswami (2006), 16 Procrustes-aligned landmarks per species were used to calculate a 16 x 16 vector dot product-moment covariance-variance matrix, using the following formula (Note: this analysis differs from Goswami in that they calculated matrix per species whereas I found the mean for each species prior to this step):

$$C_{ii'} = \frac{1}{N-1} \sum_j (\vec{x}_{ij} - \vec{u}_i) \cdot (\vec{x}_{i'j} - \vec{u}_{i'})$$

Where i is each landmark, j is each species mean, i' is each comparison landmark, $\vec{x}$ is the vector coordinates for the ith landmark of the jth individual, and $\vec{u}$ is the mean vector coordinates for the ith landmark. The resulting covariance-variance matrix was converted into a correlation matrix following the formula:

$$Corr(i, i') = \frac{Cov(i, i')}{\sqrt{Var(i)Var(i')}}$$

To identify cranial modules, the correlation matrix was then used for cluster analysis following Ward's method of linkage with the package **pvclust** in R (Suzuki and Shimodaira 2006). Cluster significance was also determined at the level of $\alpha = 0.05$ by running 1,000 iterations of a multiscale bootstrap resampling analysis in the **pvclust** package. The hypotheses tested at each tree node were as outlined in Kimes et al. 2017:

H_0: the cluster does not exist.

H_1: the cluster exists.

The **pvclust** package calculates two separate p-values for each clustering branch: an approximately unbiased (AU) value, and a bootstrap probability (BP) value (Suzuki and Shimodaira 2006, Kimes et al. 2017). The AU significance test method uses multi-step and multi-scale bootstrap resampling in which the sample sizes of the replicated datasets are changed from the original number of matrix rows (Shimodaira 2004, Kimes et al. 2017). The BP significance test method resamples the data matrix with replacement, while sample size remains uniform (Efron et al. 1996, Kimes et al. 2017). The AU value is generally considered to be less biased than the BP value (Shimodaira 2002 & 2004, Suzuki and Shimodaira 2006), and is the method used for this analysis. Finally, the correlation coefficient for each cluster was determined by calculating the average correlation for the entire cluster.

11

Once cranial modularity patterns were determined for the overall sample, Dataset A, subsamples

based on body mass were created to explore the relationship between size and cranial morphology.

The data were divided into the small Dataset B (<500g), medium Dataset C (500-8,000g), and large

Dataset D (>8,000g) body masses (Table 3). The process of Generalized Procrustes Analysis,

covariance-variance and correlation calculations, cluster analysis, and multiscale bootstrap

significance testing was subsequently reapplied to each group.

Table 3. Size groups for mass-based modular analysis. Extant mean masses from Jones et al. (2009), fossil means from Millien (2008), Vizcaino et al. eds. (2012).

Size	Species	Mean mass (g)
Small (<500g)	*Aconaemys sagei*	96.49
	Chinchilla lanigera	480.28
	Cryptomys hottentotus	75.13
	Ctenomys colburni	400
	Ctenomys dorsalis	165.6
	Ctenomys fulvus	279.88
	Ctenomys mendocinus	178.44
	Mesomys hispidus	175
	Microcavia riata	254.67
	Octodon degus	203.27
	Proechimys brevicauda	284.99
	Proechimys cuvieri	339.85
	Proechimys semispinosus	353.32
	Proechimys simonsi	284.99
	Proechimys steerei	284.99
	Spalacopus cyanus	100.86
	Steatomys pratensis	30.58
	Thrichomys apereoides	297.53
Medium (500-8,000g)	*Cavia porcellus*	727.99
	Cavia tschudii	1000
	Coendou mexicanus	2000
	Dasyprocta fuliginosa	3500.02
	Dasyprocta punctada	2309.12
	Erethizon dorsatum	7419.46
	Lagidium peruanum	1220
	Lagidium viscacia	1539.99
	Lagostomus maximus	4660.94
	Neoreomys australis (†)	7500

Large (>8,000g)	*Dinomys branickii*	12500
	Dolichotis patagonum	8000
	Hydrochoerus hydrochaeris	48144.91
	Josephoartigasia monesi (†)	> 349266

<u>*Modules by Family*</u>

In addition to body mass groupings, the dataset was also divided by family in order to explore phylogenetic signals on cranial modules. This resulted in eight family subsets for analysis: Echimyidae, Ctenomyidae, Octodontidae, Chinchillidae, Dinomyidae, Dasyproctidae, Caviidae and Erethizontidae. Bathyergidae was not included in this analysis, as more than one species is required for consistent vector dot product-moment calculations.
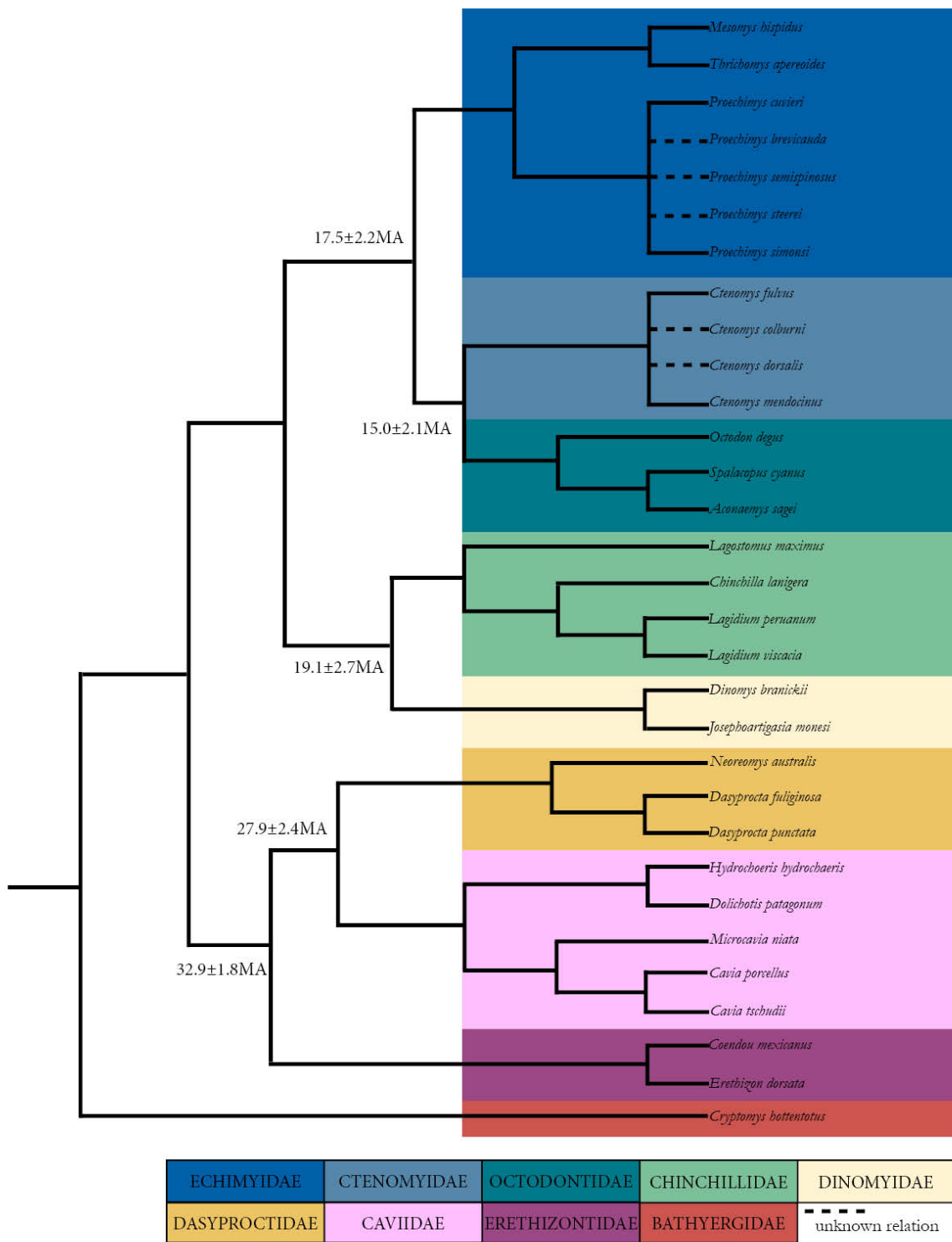
Figure 3. Phylogeny of specimens included in analysis. Species names in tree, family names color coded. Phylogenetic information from Fabre et al. (2012), divergence times from Opazo (2005).

CHAPTER III

RESULTS

Resulting clusters from each analysis are color-coded for the primary purpose of differentiation between groups within a single analysis. Because of the vast array of cluster combinations from all analyses, repeated colors in figures 4-6 do not necessarily indicate identical, but similar landmark combinations between datasets. Dataset A was used to describe modules for the entire dataset; all subsample clusters are compared to Dataset A's modules.

Dataset A: All Species

Results of this study yield five discrete modules that are generally dissimilar to those defined *a priori*: landmarks #1 and 2 form a module in the anterior-nasal region (purple; AN) (r=0.57); landmarks #4, 5 and 16 form a module spanning from the posterior end of the premaxilla to the most posterior point of the skull (vermilion; PP) (r=0.30); landmarks #6 and 7 form a module in the squamosal-jugal region (turquoise; SJ) (r=0.59); landmarks #8, 9, 10, 14 and 15 form a module spanning from the lacrimal bone to the posterior end of the frontal bone (yellow; LF) (r=0.39); landmarks #11 and 12 form a module in the occipital-tympanic region (green; OT) (r=0.74), and landmarks #3 and 13 are not associated with any modules (black). The AN module contains some of the same landmark points as the *a priori* AON module, while all other modules determined in this study appear unique to the caviomorphs. Modules calculated for size and family data subsets generally deviated from those of the overall dataset (table 4, Figure 4).

Table 4. Landmark module assignments for modular analysis of all species in analysis.

Landmark	Module
1	AN
2	AN
3	no module

Landmark	Module
4	PP
5	PP
6	SJ
7	SJ
8	LF
9	LF
10	LF
11	OT
12	OT
13	no module
14	LF
15	LF
16	PP

Dataset B: Small Species

Results for the small size subset (<500g) yield four significant modules with five landmarks falling outside of any modules (Figure II). One module (purple) matches the overall AN module identically both in landmarks (#1, 2) and in correlation (r=0.57), while SJ and OT modules are combined to form a single cluster (teal; landmarks #6, 7, 11 and 12) (r=0.41). The module in the lacrimal region of this subgroup (yellow) is different than that of the overall dataset, including only two of the five landmarks (#9, 10) (r=0.48). The final module for this subset (red) include two landmarks from the LF and one landmark from the PP module (#14, 15 and 16) (r=0.49) (Table 5, Figure 4).

Table 5. Landmark module assignments for modular analysis of small species.

Landmark	Module
1	AN
2	AN
3	no module
4	no module
5	no module
6	SJ-OT
7	SJ-OT
8	no module
9	fraction of LF fraction
10	fraction of LF
11	SJ-OT

12	SJ-OT
13	no module
14	LF-PP
15	LF-PP
16	LF-PP

Dataset C: Medium Species

Results for the medium size subset (500-8,000g) produced three significant modules with ten

landmarks falling outside of any modules (Figure II). One module (vermillion) closely resembled the

PP module from the overall dataset, including two of the same landmarks (#4, 5), but missing the

third (#16) (r=0.76). A second module (teal) included half of the landmarks from the small

subgroup's merged SJ and OT modules (#7, 12) (r=0.50), but did not resemble the modules from

the original dataset. The third (pink) module calculated for this subset does not resemble any

modules from previously described groupings, with two new landmarks clustering with a relatively

high correlation coefficient (#2, 6) (r=0.75) (Table 6, Figure 4).

Table 6. Landmark module assignments for modular analysis of medium species.

Landmark	Module
1	no module
2	fraction of AN-SJ
3	no module
4	fraction of PP
5	fraction of PP
6	fraction of AN-SJ
7	fraction of SJ-OT
8	no module
9	no module
10	no module
11	no module
12	fraction of SJ-OT
13	no module
14	no module
15	no module
16	no module

Results for the large subset (>8,000g) yield the most integrated cranial pattern amongst all groups, with all 16 landmarks divided into three distinct modules. The lacrimal region module (yellow) bears the most similarity to the original LF module, with three of the original five landmarks (#8, 9, 10), but also includes additional landmarks that were not grouped with LF landmarks (#3, 4, 5, 11, 16) (r=0.33). A second module (blue) bears very little similarity to modules calculated for datasets A-C, but includes the entirety of the AN and SJ landmarks from Dataset A, and two landmarks from the LF module (#14, 15) (r=0.49). The final module (green) for Dataset D is formed by very high correlation between two landmarks not associated in datasets A-C (#12, 13) (r=0.79) (Table 7, Figure 4).

Table 7. Landmark module assignments for modular analysis of large species.

Landmark	Module
1	AN-SJ-fraction of LF
2	AN-SJ-fraction of LF
3	PP-fraction of LF
4	PP-fraction of LF
5	PP-fraction of LF
6	AN-SJ-fraction of LF
7	AN-SJ-fraction of LF
8	PP-fraction of LF
9	PP-fraction of LF
10	PP-fraction of LF
11	PP-fraction of LF
12	fraction of OT
13	fraction of OT
14	AN-SJ-fraction of LF
15	AN-SJ-fraction of LF
16	PP-fraction of LF

Results for the Echimyidae family indicate two significant modules that incorporate all 16 landmarks (Figure III). One module (blue) is a partial fusion of the AN, SJ, OT and PP modules, including both AN landmarks (#1, 2), one of two SJ landmarks (#6), one of two OT landmarks (#12), and one of three PP landmarks (#16), as well as one typically unintegrated landmark (#13) (r=0.43). The other module (yellow) bears some resemblance to the LF module, including all original landmarks (#8, 9, 10, 14, 15), as well as the majority of the PP landmarks (#4, 5), the other half of the SJ and OT landmarks (#7, 11, respectively), and the other typically unintegrated landmark (#3) (r=0.28) (Table 8, Figure 5).

Table 8. Landmark module assignments for modular analysis of Echimyidae family.

Landmark	Module
1	AN-fractions of SJ-OT-PP
2	AN-fractions of SJ-OT-PP
3	LF-fractions of SJ-OT-PP
4	LF-fractions of SJ-OT-PP
5	LF-fractions of SJ-OT-PP
6	AN-fractions of SJ-OT-PP
7	LF-fractions of SJ-OT-PP
8	LF-fractions of SJ-OT-PP
9	LF-fractions of SJ-OT-PP
10	LF-fractions of SJ-OT-PP
11	LF-fractions of SJ-OT-PP
12	AN-fractions of SJ-OT-PP
13	AN-fractions of SJ-OT-PP
14	LF-fractions of SJ-OT-PP
15	LF-fractions of SJ-OT-PP
16	LF-fractions of SJ-OT-PP

Dataset F: Ctenomyidae Family

Cluster analysis of the Ctenomyidae data subset suggests the presence of four significant modules that incorporate 14/16 landmarks. This family possesses the SJ module (turquoise; landmarks #6, 7)

(r=0.87), the AN module plus two additional landmarks (purple; landmarks #1, 2, 5, 13) (r=0.66), the majority of the LF module (yellow; landmarks #8, 9, 10) (r=0.61), the remaining points of the LF module (red; landmarks #14, 15) (r=0.94), and a module not resembling any from the original dataset (lavender; landmarks #3, 4, 11) (r=0.60). Landmarks #10 and 12 are unassociated with any significant modules in this family (Table 9, Figure 5).

Table 9. Landmark module assignments for modular analysis of Ctenomyidae family.

Landmark	Module
1	AN-fraction of PP
2	AN-fraction of PP
3	fractions of PP-OT
4	fractions of PP-OT
5	AN-fraction of PP
6	SJ
7	SJ
8	fractions of LF-PP
9	fractions of LF-PP
10	no module
11	fractions of PP-OT
12	no module
13	AN-fractions of SJ-OT-PP
14	fraction of LF
15	fraction of LF
16	fractions of LF-PP

Dataset G: Octodontidae Family

Results for the Octodontidae family yield four significant cranial modules that include 13/16 landmarks (Figure III). The AN module matches that of the original dataset (purple; landmarks #1, 2) (r=0.95), while another cluster contains components of modules LF and PP (magenta; landmarks #4, 15) (r=0.88), and another cluster resembles the majority of the original LF module, with two additional significantly correlated landmarks (yellow; #7, 8, 9, 10, 14, 15) (r=0.47). Similar to the fourth module in the Ctenomyidae analysis, Octodontidae also has a module that does not resemble

any from the original dataset, containing landmarks #3, 5, 11 (lavender) (r=0.75) (Table 10, Figure 5).

Table 10. Landmark module assignments for modular analysis of Octodontidae family.

Landmark	Module
1	AN
2	AN
3	fractions of PP-LF
4	fractions of PP-LF
5	fraction of PP-LF
6	no module
7	fractions of SJ-LF-PP
8	fractions of SJ-LF-PP
9	fractions of SJ-LF-PP
10	fractions of SJ-LF-PP
11	fractions of PP-LT
12	no module
13	no module
14	fraction of LF
15	fraction of PP-LF
16	fractions of SJ-LF-PP

Dataset H: Chinchillidae Family

Results for the Chinchillidae family analysis indicate two significant modules that incorporate all 16 landmarks. One cluster is a combination of the original AN and OT landmarks, plus one landmark that was originally unincorporated (purple; landmarks #1, 2, 11, 12, 13) (r=0.75). The second cluster is a combination of PP, SJ and LF landmarks, as well as one originally unincorporated landmark (yellow; landmarks #3, 4, 5, 6, 7, 8, 9, 10, 14, 15) (r=0.20) (Table 11, Figure 5).

Table 11. Landmark module assignments for modular analysis of Chinchillidae family.

Landmark	Module
1	AN-OT
2	AN-OT
3	PP-SJ-LF
4	PP-SJ-LF

5	PP-SJ-LF
6	PP-SJ-LF
7	PP-SJ-LF
8	PP-SJ-LF
9	PP-SJ-LF
10	PP-SJ-LF
11	AN-OT
12	AN-OT
13	AN-OT
14	PP-SJ-LF
15	PP-SJ-LF
16	PP-SJ-LF

Dataset I: Dinomyidae Family

Results indicate two significant modules that incorporate all 10/16 landmarks in the dinomyid cranium. One cluster (teal) is a fusion of half of the landmarks in the AN, SJ and OT module (#2, 7, 12) (r=0.99). The second cluster (blue) is a combination of the remaining landmarks in the AN and SJ modules, and one component of the LF module (landmarks #1, 6, 15) (r=0.98). The third cluster (lavender) resembles the majority of the lavender clusters seen in Ctenomyidae and Octodontidae (landmarks #3, 11) (r=0.99). The final cluster (vermilion) contains the majority of the PP module landmarks (#4, 16) (r=0.98) (Table 12, Figure 6).

Table 12. Landmark module assignments for modular analysis of Dinomyidae family.

Landmark	Module
1	fractions of AN-SJ-LF
2	fractions of AN-SJ-OT
3	fraction of SJ
4	fration of PP
5	no module
6	fractions of AN-SJ-LF
7	fractions of AN-SJ-OT
8	no module
9	no module
10	no module
11	fraction of SJ
12	fractions of AN-SJ-OT

13	no module
14	no module
15	fractions of AN-SJ-LF
16	fraction of PP

Dataset J: Dasyproctidae Family

Results for the Dasyproctidae cluster analysis reveal five significant modules that include 14/16 landmarks. One cluster matches the SJ module (turquoise; landmarks #6, 7) (r=0.90), while the majority of the LF module is split into two discrete clusters: the lacrimal region (yellow; landmarks #9, 10) (r=0.91) and the frontal-parietal region (blue; landmarks #14, 15) (r=0.75). The last component of the LF module is grouped with the OT module and half of the AN module (purple; landmarks #2, 8, 11, 12) (r=0.69). The final module is a fusion of most of the PP module with an originally ungrouped landmark (vermillion; landmarks #4, 5, 13, 16) (r=0.82) (Table 13, Figure 6).

Table 13. Landmark module assignments for modular analysis of Dasyproctidae family.

Landmark	Module
1	no module
2	OT-fractions of AN-LF
3	no module
4	PP
5	PP
6	SJ
7	SJ
8	OT-fractions of AN-LF
9	fraction of LF
10	fraction of LF
11	OT-fractions of AN-LF
12	OT-fractions of AN-LF
13	PP
14	fraction of LF
15	Fraction of LF
16	PP

Cluster analysis of the caviids divides 16/16 landmarks into two significant modules. One cluster

(yellow) is a combination of the entire LF module and the majority of the PP module (landmarks

#4, 5, 8, 9, 10, 14, 15) ($r=0.40$), while the other cluster (purple) contains the rest of the PP module,

the entire AN SJ, and OT modules, and both originally unincorporated landmarks (#1, 2, 3, 6, 7, 11,

12, 13, 16) ($r=0.26$) (Table 14, Figure 6).

Table 14. Landmark module assignments for modular analysis of Caviidae family.

Landmark	Module
1	AN-SJ-OT-fraction of PP
2	AN-SJ-OT-fraction of PP
3	AN-SJ-OT-fraction of PP
4	LF-fractions of PP
5	LF-fractions of PP
6	AN-SJ-OT-fraction of PP
7	AN-SJ-OT-fraction of PP
8	LF-fractions of PP
9	LF-fractions of PP
10	LF-fractions of PP
11	AN-SJ-OT-fraction of PP
12	AN-SJ-OT-fraction of PP
13	AN-SJ-OT-fraction of PP
14	LF-fractions of PP
15	LF-fractions of PP
16	AN-SJ-OT-fraction of PP

Dataset L: Erethizontidae Family

Results indicate that the Erethizontidae family has two significant modules that incorporate all 16

landmarks. One cluster contains the majority of the LF and PP modules, and half of the AN module

(blue; landmarks #1, 8, 5, 14, 15, 16) ($r=0.82$), while the other is comprised of all remaining

landmarks, including the complete SJ and OT modules (lavender; landmarks #2, 3, 4, 6, 7, 9, 10, 11,

12, 13) ($r=0.26$) (Table 15, Figure 6).

Table 15. Landmark module assignments for modular analysis of Erethizontidae family.

Landmark	Module
1	Fractions of AN-LF-PP
2	SJ-OT-fractions of PP-LF
3	SJ-OT-fractions of PP-LF
4	SJ-OT-fractions of PP-LF
5	Fractions of AN-LF-PP
6	SJ-OT-fractions of PP-LF
7	SJ-OT-fractions of PP-LF
8	Fractions of AN-LF-PP
9	SJ-OT-fractions of PP-LF
10	SJ-OT-fractions of PP-LF
11	SJ-OT-fractions of PP-LF
12	SJ-OT-fractions of PP-LF
13	SJ-OT-fractions of PP-LF
14	Fractions of AN-LF-PP
15	Fractions of AN-LF-PP
16	Fractions of AN-LF-PP

Results Summary

Overall, modules for body mass groupings were the most strongly integrated in the large-sized data subset, moderately in the small-sized data subset, and weakly in the medium-sized dataset. Sample size does not have an obvious effect on these results, with the small-sized group having 18 species means, the medium 10 species means, and the large 4 species means.

Families Echimyidae, Chinchillidae, Caviidae and Erethizontidae have the most integrated crania, Ctenomyidae, Octodontidae and Dasyproctidae have moderately integrated crania, and Dinomyidae has the poorest cranial integration. Sample size may play a small part in this discrepancy, as the most highly integrated groups have the highest number of species means incorporated, and the most poorly integrated group has just 2 species means. However, other factors are also likely at play, as one highly integrated group also has two species means. There is no clear pattern relating the age of a lineage to its level of cranial integration.
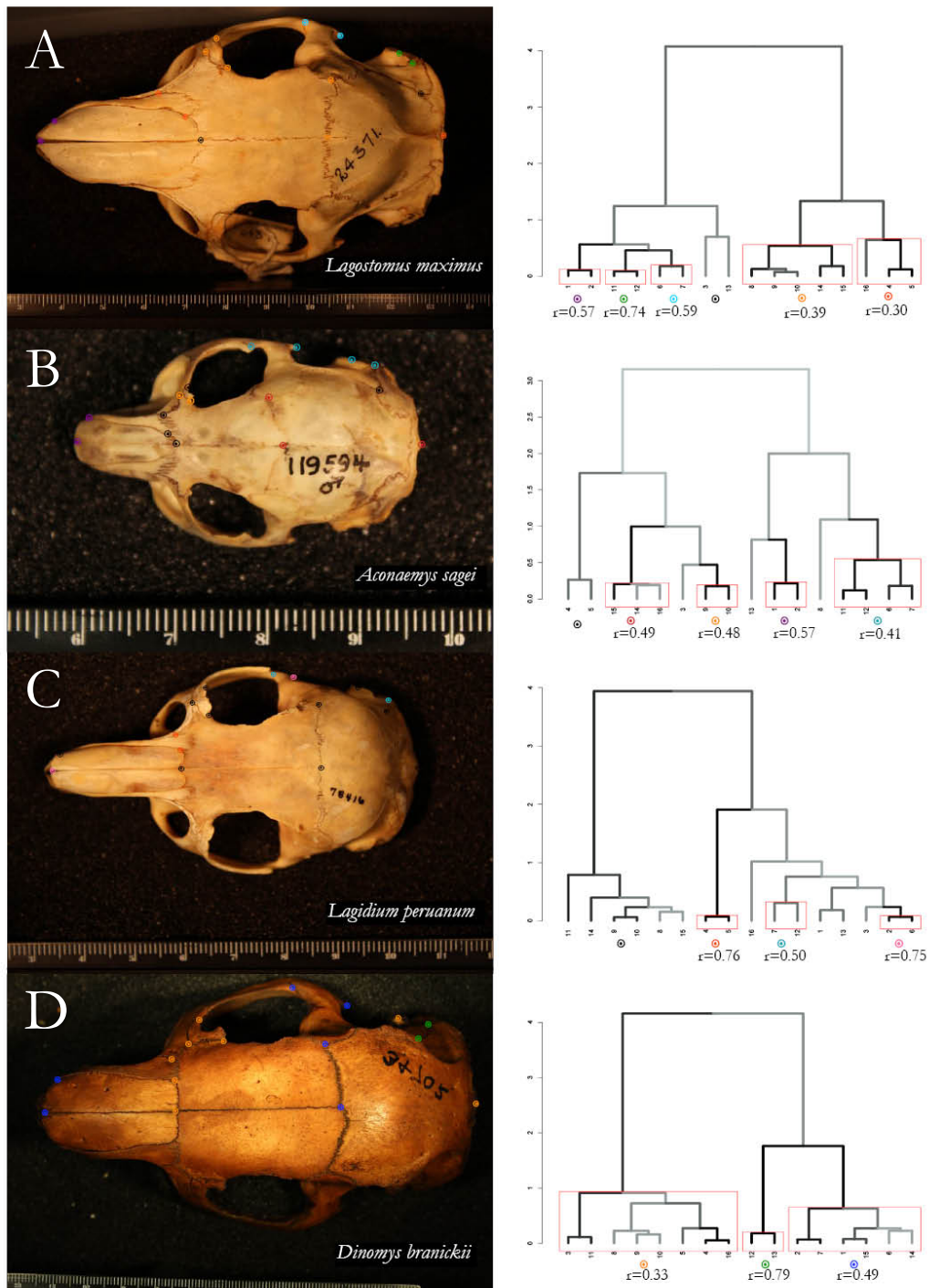
Figure 4. Dorsal cranial modules of datasets A-D. (A) Dataset A: complete dataset, (B) Dataset B: small body mass, (C) Dataset C: medium body mass, (D) Dataset D: large body mass. Red boxes indicate AU significance, grey to black branch color gradient indicates BP significance.
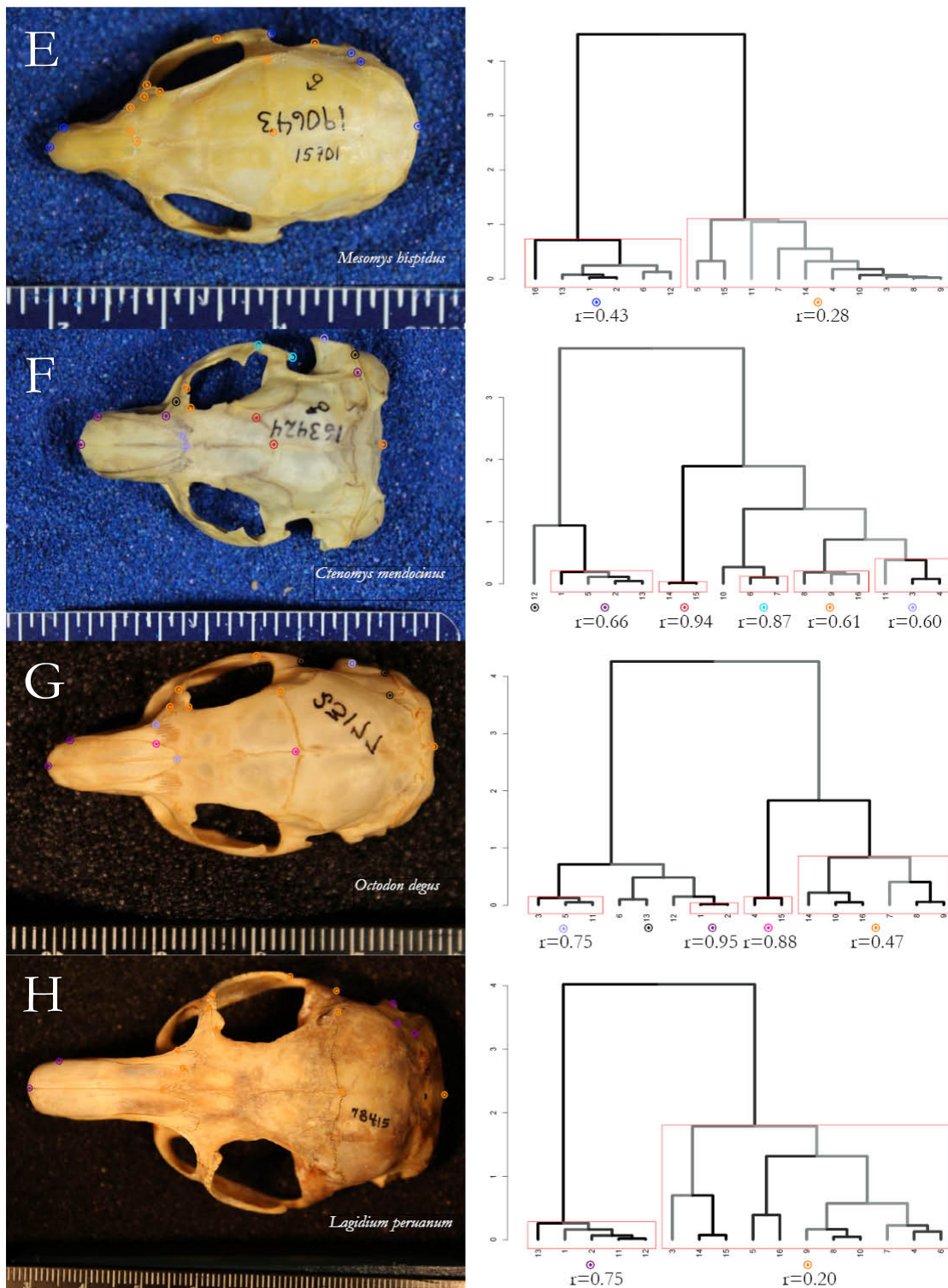
Figure 5. Dorsal cranial modules of datasets E-H. (E) Dataset E: Echimyidae, (F) Dataset F: Ctenomyidae, (G) Dataset G: Octodontidae, (H) Dataset H: Chinchillidae. Red boxes indicate AU significance, grey to black branch color gradient indicates BP significance.

27
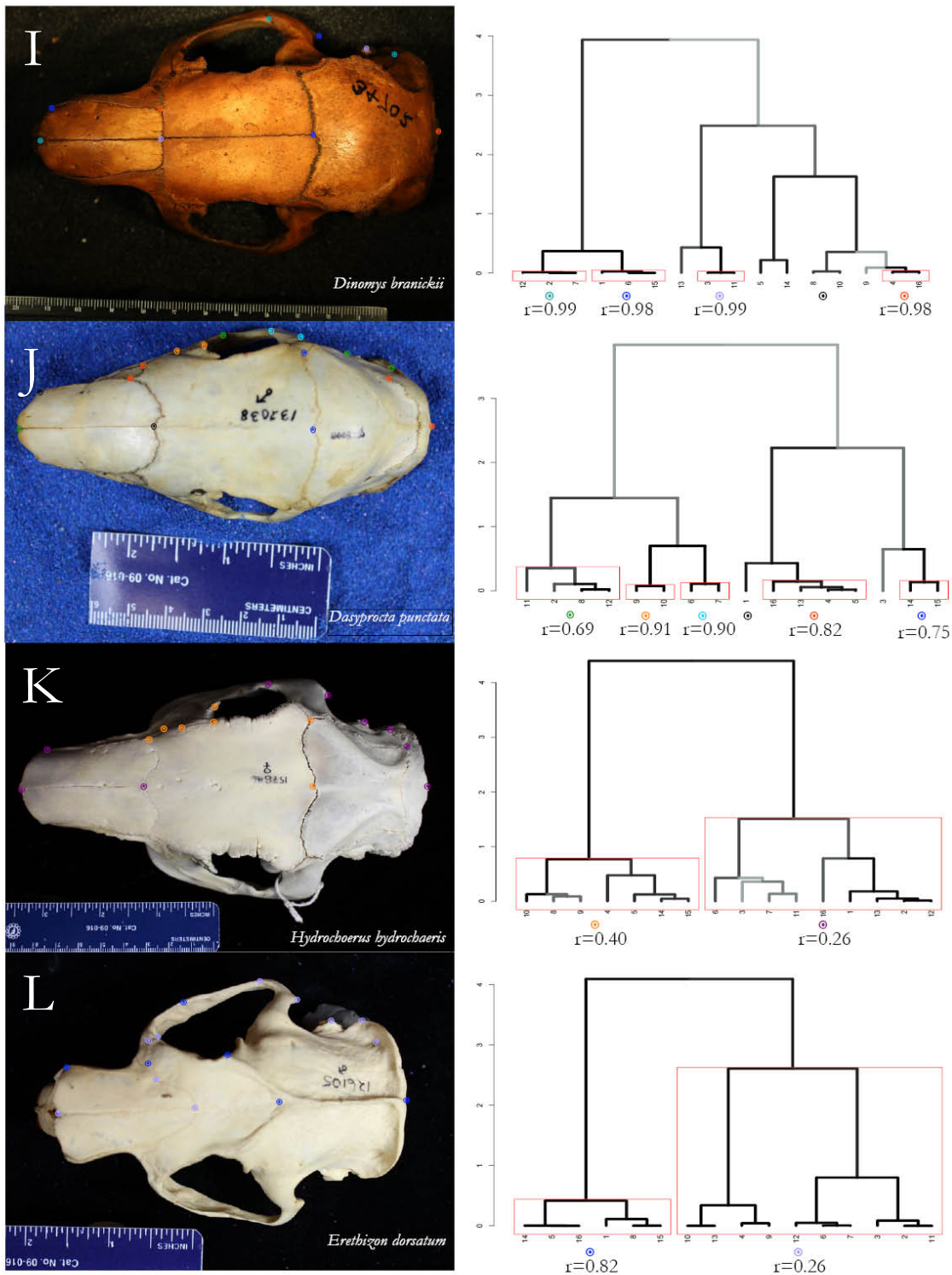
Figure 6. Dorsal cranial modules of datasets I-L. (I) Dataset I: Dinomyidae, (J) Dataset J: Dasyproctidae, (K) Dataset K: Caviidae, (L) Dataset L: Erethizontidae. Red boxes indicate AU significance, grey to black branch color gradient indicates BP significance.

CHAPTER IV

DISCUSSION

Results of this study indicate that dorsally visible cranial caviomorph modules deviate from *a priori* mammalian module descriptions. While the anterior-nasal module determined in this study contains similarities with previous literature (AON module; Goswami 2006, Goswami and Polly 2010), all other modules are unique to the caviomorph group. Datasets divided by body size show that high cranial integration corresponds to low ecological diversity, indicating modular constraint on diversification. With the exception of Dasyproctidae and Erethizontidae, datasets divided by family do not exhibit such a simple pattern. Echimyidae, Chinchillidae and Caviidae show a correlation between high cranial integration and high morphological diversity, indicating modular facilitation of diversification. Ctenomyidae, Octodontidae and Dinomyidae exhibit no clear patterns of modular facilitation or constraint.

Dataset A

The AN module found in the overall dataset indicates that, as seen for other mammals, points within the anterior nasal region of the dorsal cranium are highly correlated with one-another, functionally corresponding with the masticatory apparatus of the skull (Goswami 2006). The landmarks composing the PP module do not correspond directly with a traditional functional unit, but do suggest that the shape of the posterior region of the premaxilla is related to the location of the posterior end of the skull. In previous literature, the premaxilla is considered part of the Anterior-Oral-Nasal module (Goswami 2007). This dataset indicates that, for caviomorphs, the premaxillary component of the masticatory apparatus is functionally linked to changes at the posterior region of the cranium, likely related to the changing pattern of masseter musculature, and the associated cranial stress exerted by chewing with molars. The SJ module is located at the

29

posterior end of the zygomatic arch, and is also a component of the masticatory apparatus, experiencing the highest amount of strain during mastication (Goswami 2007). While the AN, PP and SJ modules are all components of the same functional group, this dataset suggests that the anterior nasal region, posterior premaxilla region, and posterior zygomatic region do not covary significantly as one module, but appear to be independent units.

The LF module includes all lacrimal points used in this analysis, as well as the sutures between the frontal and parietal bones. The lacrimal region is similar to the *a priori* orbit module in published literature (Goswami and Polly 2010), and is where the visual sensory organs are located (Goswami 2006). In contrast, the suture between frontal and parietal bones is part of the Cranial Vault (CV) module in previous literature (Goswami and Polly 2010), which provides protection and support for the brain (Goswami 2006). While the correlation between the lacrimal points and the posterior end of the frontal bone is inconsistent with other findings, for caviomorphs, there appears to be a relationship between the shape of visual sensory organs and the shape of the brain case. Similar to the *a priori* CV module, the OT module is in a region that provides support and protection for the brain (Goswami 2006). This module includes the external auditory meatus, which is highly correlated with the nearby squamosal-occipital-tympanic suture, and not significantly correlated with other protective regions surrounding the brain.

Modules by Body Size

The small caviomorph dataset is represented by diverse ecologies, containing species that are epigean, arboreal, and fossorial to subterranean (Myers ADW, Red List). Analysis of this dataset indicates the presence of four significant modules that incorporate 11/16 landmarks (Figure 4). Within this group, the AN module (purple) appears to be highly conserved, while the SJ and OT modules are merged to form a single cluster (teal). The LF module is reduced to form a smaller

30

cluster (yellow) while the fourth cluster (red) is a combination of other LF and PP landmarks. The AN module for this dataset indicates a moderate functional constraint on the anterior-nasal region of the masticatory apparatus (Goswami 2007), while another component of the masticatory apparatus, the SJ module, has a moderately weak correlation with the OT module of the cranial vault region (check this), which provides protection to the brain (Goswami 2006). This indicates independence between anatomical points linked to mastication, and a link between zygomatic structure and morphology along the peripheral cranial vault. The reduced LF module within this group suggest that while the lacrimal region may change shape, the moderate correlation between certain lacrimal points remains critical to the visual sensory system around the orbit (Goswami 2007). The last cluster (red) does not closely resemble any module from the overall dataset, but suggests a moderate correlation between frontal-parietal cranial vault landmarks and the posterior point of the skull. The moderate correlation values accompanied by the moderate level of integration are reflective of a moderate range of morphological and ecological diversity within the small caviomorphs.

Ecologies for the medium group are very broad, spanning epigean, cursorial, fossorial and arboreal lifestyles (Red List, Myers ADW). This group yields poorly integrated crania with three significant modules, two of which do not closely resemble the modules from dataset A (Figure 4). One cluster contains the rostral region of the PP module (vermillion), while a second cluster contains half of the SJ and OT landmarks (teal), and a third cluster contains half of the AN and SJ landmarks (pink). This dataset represents a decoupling of the AN, SJ and OT modules and replacement by new landmark associations, indicating a general lack of constraint from these modules on morphological and ecological diversification. However, the persistent correlation of the PP module suggests morphological importance of the posterior rostral region for the masticatory apparatus within this size group.

The large caviomorphs in this study are epigean and semiaquatic. This dataset indicates highly integrated crania amongst large caviomorphs, with three clusters encompassing all landmarks (Figure 4). The yellow module is a combination of the PP module, a nearly completely intact LF module, and two additional landmarks with relatively low mean correlation. The green cluster does not resemble any established from dataset A and exhibits moderately high correlation, while the blue cluster represents a moderately correlated combination of AN, SJ, and the remaining LF landmarks. The yellow cluster represents a linkage, however weak, between the morphology of the visual sensory organ, the posterior rostral masticatory region, the auditory canal and the posterior end of the skull. The blue cluster indicates a moderate correlation between masticatory modules AN and SJ, as well as with the frontal-parietal region of the cranial vault. The high level of cranial integration within large caviomorphs appears to be associated with a lower level of ecological diversity in comparison to the small and medium datasets.

The modules belonging to each size grouping generally did not match modules found for the overall dataset. However, some patterns were pervasive throughout each group. With the exception of the medium size group, all datasets indicated correlation between AN landmarks, and with the exception of the small size group, all datasets also indicated correlation between rostral components of the PP module. The SJ module from dataset A is intact in the small and large caviomorph groupings, although in both latter cases, other landmarks are incorporated into the module. The LF module is fragmented in all data subsets, represented only by landmarks #9 and 10 for small caviomorphs, no landmarks for medium caviomorphs, and landmarks #8, 9 and 10, among other landmarks not linked to the original LF module, for large caviomorphs. The remaining landmarks #14 and 15 are significantly correlated for small and large caviomorphs, but fall within clusters that differ both from each other and from the overall analysis. The OT module occurs only in the small subset but differs

in being significantly correlated to the SJ module landmarks. With the exception of the large caviomorphs dataset, landmarks #3 and 13 consistently fell outside of any significant clusters.

Overall, the small caviomorphs showcase moderate cluster correlations and moderate degree of integration, the medium caviomorphs have relatively high cluster correlations and a low level of integration, and the large caviomorphs have a broad range of correlation values and a high degree of integration. These findings indicate that crania of large-sized caviomorphs are the most integrated, while those of medium sized caviomorphs are the least integrated, with crania of small-sized caviomorphs exhibiting a moderate amount of integration. When considering the ecological breadth of each group, the high level of integration within large caviomorph crania is correlated with the most specialized group, while the moderate integration of the small and medium size groups is correlated with more ecologically diverse groups. These findings loosely support the size-based component of my hypothesis: large-sized caviomorphs have more highly integrated cranial systems to accompany their lower level of ecological diversity, while the smaller two groups possess less integrated crania and exhibit higher levels of ecological diversity. However, between the small and medium groups, the pattern does not support my hypothesis: while both size groups contain arboreal, fossorial and epigean ecologies, the medium-sized group is less integrated.

Modules by Phylogeny

The Echimyidae family has a shallow phylogenetic divergence, occurring about 17.5 Ma (Opazo 2005). Their crania possess large auditory bullae and delicate zygomatic arches (Myers ADW). Analysis reveals two discrete significant clusters with low to medium correlation, indicating landmarks with moderate influence over one another within the blue module, most of which are proximal points ($r=0.43$), and low influence over one another within the yellow module, most of which are distal points ($r=0.28$). The two clusters include all 16 landmarks, indicating highly

integrated crania. However, the correlation coefficients suggest that while highly integrated, the landmarks within each respective module, on average, only have a small relationship to one another. This result suggests that for Echimyidae crania, a moderately shallow phylogenetic divergence is associated with high cranial integration.

Ctenomyidae is a group of caviomorphs with a shallow phylogenetic divergence occurring 15 Ma (Opazo 2005). They possess broad, flat crania, broad rostra, wide and bowed zygomatic arches, parietal ridges, and no sagittal crests (Myers ADW). The Ctenomyidae modules determined in this study reflect this morphology, containing both uncorrelated and highly correlated sets of landmarks, with relatively high integration of five significant modules. This group possesses the original SJ module (turquoise) with a high degree of correlation, indicating a high degree of influence between landmarks in the zygomatic region. Another highly correlated pair of landmarks are the squamosal-parietal components of the original LF module (vermillion), indicating dependence between traits within the cranial vault. The other modules, which encompass the rostral region (purple, lavender), components of the lacrimal region (yellow), and the posterior of the skull (yellow) all have moderately high correlation values, suggesting a smaller, but still considerable level of dependence between landmarks in their respective modules throughout the family. These results suggest that within Ctenomyidae, a shallow divergence time is linked to a high level of cranial integration.

Octodontidae is a family of caviomorphs that split from Ctenomyidae roughly 15 Ma (Opazo 2005). Skulls in this family are typically short and angled with simple zygomatic arches, and in many species, the bullae are significantly enlarged (Myers ADW). In this study, octodontids exhibit a moderately high level of cranial integration, in a total of four significant modules. The AN module (purple) and a new cluster (magenta) are both highly correlated in this family, and are components of the rostrum and cranial vault, respectively. These modules represent the most highly dependent sets

of landmarks within the family, indicating that changes in traits within each module are highly dependent upon one another, influencing their evolutionary change. Another new moderately highly correlated module (lavender) represents a dependent relationship between parts of the rostrum and the external auditory meatus. The majority of the LF module is intact, with two additional landmarks, indicating a moderately correlated relationship between the lacrimal region, components of the zygomatic and cranial vault regions, and the posterior point of the skull. In this family, shallow phylogenetic divergence is associated with moderately high cranial integration.

Chinchillidae evolved roughly 19 Ma (Opazo 2005). The chinchillid cranium has a significantly enlarged infraorbital foramen, an enlarged lacrimal with the lacrimal canal opening on the side of the rostrum, enlarged to significantly enlarged auditory bullae, and reduced zygomatic plates (Myers ADW). Results reveal that chinchillid crania are highly integrated, with low to moderately high correlation values. One module (purple) encompasses peripheral points of the cranium, specifically the AN and OT landmarks with a relatively high degree of correlation (r=0.75), suggesting a functional link between the anterior region of the masticatory apparatus and the cranial vault (Goswami 2006, 2007). Conversely, the weakly correlated yellow module consists of all remaining landmarks including the entire LF, PP and SJ modules, indicating a small amount of dependence between cranial vault and the posterior rostral and zygomatic areas. Results suggest that the moderate depth of divergence within this family corresponds to a high degree of cranial integration.

Dinomyidae is a family that diverged 19 Ma (Opazo 2005). Results indicate dinomyid crania have a relatively low level of integration and exceptionally highly correlated modules. Most of the modules from the original dataset are decoupled in this family, with the exception of two PP landmarks, but the clusters found indicate strong morphological links between points that are spatially distant from one another, completely unique to this family, and with no decipherable pattern. The moderate

depth of phylogenetic divergence is associated with notably high modular correlation values within a poorly integrated cranial system.

Dasyproctidae is a family of caviomorph rodents that evolved roughly 28 Ma (Opazo 2005). Their crania are relatively elongate, with delicate zygomatic arches and premaxillae and nasals that extend anteriorly past the incisors (Myers ADW). Results of this study reveal a relatively highly integrated cranial system with five highly correlated clusters. The SJ (turquoise) module is intact, as are the PP (vermillion) and OT (green) modules, although both of the latter contain additional landmarks not present in the original dataset. The LF module is split between green, yellow and blue clusters, while the AN module is decoupled in this dataset. The majority of clusters in this dataset loosely agree with the modules from the overall dataset, suggesting traditional functional roles within the masticatory, cranial vault and orbit regions. The exception to this trend is the absence of the AN module, indicating a decrease in functionality of the strong correlation between the anterior nasal region. The relatively deep phylogenetic divergence can be linked to a fairly high level of cranial integration in this family.

Caviidae is a family that evolved 28 Ma (Opazo 2005), and typically possess crania with well-developed bullae (Gorog and Myers ADW). This study showcases a highly integrated cranial pattern within the caviid group, with all landmarks incorporated into two relatively weakly correlated modules. The moderately weakly correlated yellow cluster contains all LF landmarks, as well as the rostral components of the PP module, suggesting a degree of dependence between the posterior rostral region of the masticatory apparatus and the orbital region of the visual-sensory system. The weakly correlated purple cluster includes the complete AN, SJ and OT modules, along with all remaining landmarks, indicating a small degree of linkage between the morphology of the rostral and zygomatic regions of the masticatory function, the peripheral region of the cranial vault and the

auditory meatus. Within this family, a deep phylogenetic divergence corresponds to high cranial integration.

Erethizontidae caviomorphs evolved 33 Ma (Opazo 2005). This family's crania possess substantial zygomatic arches, significantly large infraorbital canals, and enlarged auditory bullae, as they have exceptional hearing but bad vision (Gorog and Myers ADW). This family possesses highly integrated crania, with all landmarks being incorporated into two significant clusters. The AN, PP and LF modules are decoupled in this dataset, split between the strongly correlated blue cluster and the weakly correlated lavender. However, both the SJ and OT modules are intact within the poorly correlated lavender cluster, indicating a small degree of dependence between distal points of the cranial vault and the zygomatic component of the masticatory apparatus. This family has the deepest phylogenetic divergence studied in this data set, and is associated with a high level of cranial integration.

In general, results of this analysis do not support the phylogenetic aspect of my hypothesis. The three families with the deepest phylogenetic divergences in this analysis (Erethizontidae; 32.9 Ma, Dasyproctidae; 27.9 Ma and Caviidae 27.9 Ma, Opazo 2005) contradicted my hypothesis by all having moderately to highly integrated crania. Two of three families with moderate depth of divergence also possessed highly integrated crania (Chinchillidae; 19.1 Ma and Echimyidae, 17.5 Ma, Opazo 2005), while the third family had poorly integrated crania (Dinomyidae; 19.1 Ma, Opazo 2005). The families with the shallowest divergences (Octodontidae; 15.0 Ma and Ctenomyidae; 15.0 Ma Opazo 2005) both had moderate cranial diversity, further failing to support my hypothesis.

In failing to support my hypothesis, these results indicate that modularity does not become more constrained in shallower lineages for the caviomorph radiation, but that cranial modularity can be well or poorly integrated regardless of phylogenetic depth of divergence. If specialization is

occurring in these groups, the specialized morphologies aren't detected with my methods. One explanation is that more landmarks, or a higher sample size, could more clearly emphasize the modular patters associated with phylogenetic divergence, but it is also possible that in this lineage, integration is not strongly tied to morphological specialization as hypothesized.

<center>*Future Directions*</center>

In future studies, it will be important to incorporate improved methods for landmarking error compensation. For the sake of expedient data collection, only the right half of the dorsal cranium was landmarked, under the assumption that landmarking both sides of each skull would produce redundant data in a bilaterally symmetrical system (Cardini et al. 2005, Cardini 2016, Álvarez et al. 2013). However, recent research indicates that landmarking both sides of bilaterally symmetrical structures can provide a more complete picture of morphological patterns of the structures in question (Cardini 2016). When mirrored structures form small asymmetries during development, variation on one side will differ from, and be dependent on, variation on the other side (Cardini 2016). Consequently, measuring just one side of such a structure risks losing important and available information. It is recommended that to enhance accuracy as well as visualization, both sides of a bilaterally symmetrical structure be landmarked, and in the case of missing data, the complete side of the structure be mirror-reflected (Cardini 2016).

Three-dimensional anatomical measurements are critical to understanding the processes and patterns of a three-dimensional system. However, current methods for three-dimensional data collection of large numbers of specimens are limited by time, portability and cost (Olsen and Westneat 2015). Collecting three-dimensional cranial data from three different museums for this project was not feasible. Instead, a DSLR camera was used to collect two-dimensional data of dorsal, ventral, lateral and ventral aspects of each specimen. Limited by time, this project only provides a preview of the

<center>38</center>

modular information this data has the potential of providing. The data we currently possess can be converted into more useful biological information by transforming multiple two-dimensional aspects of a specimen into one three-dimensional object using the 'unifyVD.R' function in R (Haber 2011). This program takes two aspects of the same structure and unifies them into one set of three-dimensional landmarks using common landmarks (Haber 2011), and would enable the linkage of photographs that have already been captured at AMNH, MVZ and FMNH.

The robustness of the preliminary findings in this project can be improved by increasing the sample size of both modern and fossil specimens. Recent research on morphological integration indicates that sample sizes below N=20 are at risk of producing inaccurate correlation and significance values, and are at risk of producing false negatives and to a lesser extent, false positives (Garland et al. 2017). Future studies should aim to create larger sample sizes. More specimens can be collected from published literature, museum collections, and through international research contacts.

CHAPTER V

CONCLUSION

This study represents a preliminary analysis of cranial modularity of caviomorph rodents. Results suggest that caviomorphs exhibit a unique pattern of modularity compared to other mammalian orders studied, with the only similar module consisting of points in the anterior-nasal region. Within the data subsets divided by mass, high levels of integration loosely correspond to lower levels of ecological diversity. The large mass subset exhibited the highest level of integration, with the least ecological diversity, while the small and medium mass groups had lower levels of integration and an increase in ecological diversity. Within the data subsets divided by family, the same general pattern is not observed. The families with the deepest divergences have higher or similar levels of integration to those with the shallowest divergences, indicating that cranial morphology is not constrained by phylogenetic history. Overall, results show that while caviomorphs clearly have unique cranial morphological patterns, no simple model yet exists to explain the relationship between their cranial modularity, integration, body size or phylogenetic history.

APPENDIX

SPECIMENS INCLUDED IN STUDY

Family	Species	ID	Collection	Location
Bathyergidae	*Cryptomys hottentotus*	117780	MVZ	Cape Province, South Africa
		117782	MVZ	Cape Province, South Africa
		117783	MVZ	Cape Province, South Africa
		117784	MVZ	Cape Province, South Africa
		117871	MVZ	Cape Province, South Africa
Caviidae	*Cavia porcellus*	119105	FMNH (z)	El Beni, Bolivia
		119109	FMNH (z)	El Beni, Bolivia
		119118	FMNH (z)	El Beni, Bolivia
		119119	FMNH (z)	El Beni, Bolivia
		119120	FMNH (z)	El Beni, Bolivia
	Cavia tschudii	139593	MVZ	Puno, Peru
		139594	MVZ	Puno, Peru
		139595	MVZ	Puno, Peru
		139599	MVZ	Puno, Peru
		139600	MVZ	Puno, Peru
	Dolichotis patagonum	49212	FMNH (z)	Zoo (Chicago Zoological Society)
		53719	FMNH (z)	Zoo (Chicago Zoological Society)
		60481	FMNH (z)	Zoo (Lincoln Park Zoo)
		121555	FMNH (z)	Zoo (Lincoln Park Zoo)
	Hydrochoerus hydrochaeris	116818	MVZ	Darien, Panama
		116819	MVZ	Darien, Panama
		153573	MVZ	Amazonas, Peru
		157846	MVZ	Amazonas, Peru
		157847	MVZ	Amazonas, Peru
	Microcavia niata	53644	FMNH (z)	La Paz, Bolivia
		53654	FMNH (z)	La Paz, Bolivia
		53655	FMNH (z)	La Paz, Bolivia
		53658	FMNH (z)	La Paz, Bolivia
		53660	FMNH (z)	La Paz, Bolivia
Chinchillidae	*Chinchilla lanigera*	22253	FMNH (z)	Coquimbo, Chile
		22254	FMNH (z)	Coquimbo, Chile
		60614	FMNH (z)	Zoo (Chicago Zoological Society)

		178049	FMNH (z)	Zoo (Prep Lab Catalogue)
		178050	FMNH (z)	Zoo (Prep Lab Catalogue)
	Lagidium peruanum	49428	FMNH (z)	Arequipa, Peru
		52723	FMNH (z)	Puno, Peru
		52724	FMNH (z)	Puno, Peru
		78415	FMNH (z)	Puno, Peru
		78416	FMNH (z)	Puno, Peru
	Lagidium viscacia	53672	FMNH (z)	La Paz, Bolivia
		53673	FMNH (z)	La Paz, Bolivia
		53688	FMNH (z)	La Paz, Bolivia
		53692	FMNH (z)	La Paz, Bolivia
		53693	FMNH (z)	La Paz, Bolivia
	Lagostomus maximus	24371	FMNH (z)	Buenos Aires, Argentina
		53704	FMNH (z)	Zoo (Chicago Zoological Society)
		53737	FMNH (z)	Zoo (Chicago Zoological Society)
		54339	FMNH (z)	Boqueron, Paraguay
		54244	FMNH (z)	Buenos Aires, Argentina
Ctenomyidae	*Ctenomys colburni*	124519	FMNH (z)	Santa Cruz, Argentina
		124521	FMNH (z)	Santa Cruz, Argentina
		124522	FMNH (z)	Santa Cruz, Argentina
		124524	FMNH (z)	Santa Cruz, Argentina
	Ctenomys dorsalis	54347	FMNH (z)	Boqueron, Paraguay
		54391	FMNH (z)	Boqueron, Paraguay
		54392	FMNH (z)	Boqueron, Paraguay
		54396	FMNH (z)	Boqueron, Paraguay
		63868	FMNH (z)	Boqueron, Paraguay
	Ctenomys fulvus	23218	FMNH (z)	Antofagasta, Chile
		23222	FMNH (z)	Antofagasta, Chile
		23225	FMNH (z)	Antofagasta, Chile
		23792	FMNH (z)	Antofagasta, Chile
		34916	FMNH (z)	Antofagasta, Chile
	Ctenomys mendocinus	162283	MVZ	Rio Negro, Argentina
		162284	MVZ	Rio Negro, Argentina
		163424	MVZ	Rio Negro, Argentina
		163425	MVZ	Rio Negro, Argentina
		181571	MVZ	Rio Negro, Argentina
Dasyproctidae	*Dasyprocta fuliginosa*	170938	MVZ	Francisco de Orellana, Ecuador
	Dasyprocta punctada	98879	MVZ	San Miguel, El Salvador
		132035	MVZ	San Miguel, El Salvador
		132037	MVZ	San Miguel, El Salvador
		132038	MVZ	San Miguel, El Salvador
		132039	MVZ	Santa Ana, El Salvador
	Neoreomys australis(†)	P13155	FMNH (g)	Santa Cruz, Argentina

Dinomyidae	*Dinomys branickii*	24234	FMNH (z)	Pasco, Peru
		34702	FMNH (z)	Pasco, Peru
		69594	FMNH (z)	Antioquia, Colombia
		69595	FMNH (z)	Antioquia, Colombia
	Josephoartigasia monesi(†)	921	MNHN	San Jose, Uruguay
Erethizontidae	*Coendou mexicanus*	98877	MVZ	San Miguel, El Salvador
		132018	MVZ	Cuscatlan, El Salvador
		132022	MVZ	San Miguel, El Salvador
		132023	MVZ	San Miguel, El Salvador
		132024	MVZ	San Miguel, El Salvador
	Erethizon dorsatum	36363	MVZ	California, USA
		53702	MVZ	British Columbia, Canada
		99287	MVZ	California, USA
		109450	MVZ	California, USA
		126105	MVZ	California, USA
Echimyidae	*Mesomys hispidus*	190640	MVZ	Amazonas, Brazil
		190641	MVZ	Amazonas, Brazil
		190642	MVZ	Amazonas, Brazil
		190643	MVZ	Amazonas, Brazil
		190644	MVZ	Amazonas, Brazil
	Proechimys brevicauda	11258	AMNH	Florida, USA
		11262	AMNH	Florida, USA
		11297	AMNH	Puntarenas, Costa Rica
	Proechimys cuvieri	11260	AMNH	Florida, USA
		11263	AMNH	Florida, USA
		11271	AMNH	Florida, USA
		11308	AMNH	Florida, USA
		11309	AMNH	Florida, USA
	Proechimys semispinosus	164965	MVZ	Limon, Costa Rica
		164969	MVZ	San Jose, Costa Rica
		164971	MVZ	San Jose, Costa Rica
		164972	MVZ	San Jose, Costa Rica
		164973	MVZ	San Jose, Costa Rica
	Proechimys simonsi	11283	AMNH	New York, USA
		11294	AMNH	New York, USA
		11299	AMNH	Florida, USA
		268278	AMNH	Loreto, Peru
	Proechimys steerei	11278	AMNH	New York, USA
		11279	AMNH	New York, USA
		11281	AMNH	New York, USA
		11282	AMNH	New York, USA
	Thricomys apereoides	145321	MVZ	Concepcion, Paraguay
		145326	MVZ	Cordillera, Paraguay
Octodontidae	*Aconaemys sagei*	50757	FMNH (z)	La Araucania, Chile
		50760	FMNH (z)	La Araucania, Chile
		119594	FMNH (z)	La Araucania, Chile

	119596	FMNH (z)	La Araucania, Chile
	119597	FMNH (z)	La Araucania, Chile
Octodon degus	21373	FMNH (z)	Valparaiso, Chile
	22249	FMNH (z)	Valparaiso, Chile
	23177	FMNH (z)	Valparaiso, Chile
	23179	FMNH (z)	Valparaiso, Chile
	23182	FMNH (z)	Valparaiso, Chile
Spalacopus cyanus	23014	FMNH (z)	Valparaiso, Chile
	23015	FMNH (z)	Valparaiso, Chile
	23018	FMNH (z)	Valparaiso, Chile
	119605	FMNH (z)	Valparaiso, Chile
	119606	FMNH (z)	Valparaiso, Chile

Appendix. Specimens included in study. AMNH = American Museum of Natural History. FMNH = Field Museum of Natural History, geological collection (g) or zoological collection (z). MNHN = Museo Nacional de Historia Natural y Antropología. MVZ = Museum of Vertebrate Zoology.

REFERENCES CITED

Ackermann, R. R., and J.M. Cheverud. "Morphological integration in primate evolution." *Phenotypic integration: Studying the ecology and evolution of complex phenotypes* (2004): Eds. M. Pigliucci & K. Preston (pp. 302–319). Oxford: Oxford University Press.

Adams, D.C., E. Otarola-Castillo and E. Sherratt. "Geomorph: Software for geometric morphometric analyses." R package version 2.0 (2014): http://cran.r-project.org/web/packages/geomorph/index.html.

Adams, D.C., and E. Otarola-Castillo. "Geomorph: an R package for the collection and analysis of geometric morphometric shape data." *Methods in Ecology and Evolution*. 4(2013): 393-399.

Adams, D.C., Rohlf F.J. and D.E. Slice. "Geometric morphometrics: ten years of progress following the 'revolution'." *Italian Journal of Zoology* 71.1 (2004): 5–16.

Adams, D.C., Rohlf F.J., Slice D.E. "A field comes of age: geometric morphometrics in the 21st century." *Hystrix: the Italian Journal of Mammalogy* 24.1 (2013): 7–14.

Álvarez, A., Perez, I.S., and D.H. Verzi. "Ecological and Phylogenetic Dimensions of Cranial Shape Diversification in South American Caviomorph Rodents (Rodentia: Hystricomorpha)." *Biological Journal of the Linnean Society* 110 (2013): 898-913.

Álvarez, A., Perez S.I. and D.H. Verzi D.H. "The role of evolutionary integration in the morphological evolution of the skull of caviomorph rodents (Rodentia: Hystricomorpha)." *Evolutionary Biology* 42.3 (2015): 312–327.

Bolker, J.A. "Modularity in development and why it matters to evo-devo." *American Zoologist* 40 (2000): 770-776.

Cardini, A. "Lost in the Other Half: Improving Accuracy in Geometric Morphometric Analyses of One Side of Bilaterally Symmetric Structures." *Systematic Biology* 65.6 (2016): 1096-1106.

Cardini, A., Hoffmann, R.F., and R.W. Thorington Jr. "Morphological evolution in marmots (Rodentia, Sciuridae): size and shape of the dorsal and lateral surfaces of the cranium." *Journal of the Zoological Systematics and Evolutionary Research* 43 (2005): 258-268.

Cox, P. G., Rayfield, E. J., Fagan, M. J., Herrel, A., Pataky, T. C., and N. Jeffery. "Functional Evolution of the Feeding System in Rodents." *PLoS ONE*, *7*.4 (2012): e36299. http://doi.org/10.1371/journal.pone.0036299

Efron, B., Halloran, E., and S. Holmes. "Bootstrap confidence levels for phylogenetic trees." *Proceedings of the National Academy of Sciences* 93.23 (1996): 13429-13434.

Eisenberg, J. F., & Redford, K. H. *Mammals of the Neotropics. Vol. 3: the Central Neotropics—Ecuador, Peru, Bolivia, Brazil* (1999). Chicago: University of Chicago Press

Elissamburu, A., and S.F. Vizcaíno. "Limb proportions and adaptations in caviomorph rodents (Rodentia: Caviomorpha)." *Journal of Zoology London* 262.2 (2004): 145–159.

Emerson, S.B., and P.A. Hastings. "Morphological correlations in evolution: consequences for phylogenetic analysis." *Quarterly Review of Biology* 73 (1998): 141-162.

Fabre, P.H., Hautier, L., Dimitrov, D. and E.J.P. Douzery. "A glimpse on the pattern of rodent diversification: a phylogenetic approach."*BioMed Central Evolutionary Biology* 12.88 (2012): 1-19.

Flynn, J.J. and A.R. Wyss. "Recent Advances in South American Mammalian Paleontology." *Trends in Ecology & Evolution* 13.11 (1998): 449-454.

Garland, K., Marcy, A., Sherratt, E., and V. Weisbecker. "Out on a limb: bandicoot limb co-variation suggests complex impacts of development and adaptation on marsupial forelimb evolution." *Evolution & Development* 19.2 (2017): 69-84.

Gorog, T., and P. Myers. "Chinchillidae: chinchillas and viscachas." *Animal Diversity Web*. University of Michigan. Animaldiversity.org.

Gorog, T., and P. Myers. "Erethizontidae: New World porcupines." *Animal Diversity Web*. University of Michigan. Animaldiversity.org.

Goswami, A. "Cranial Modularity Shifts during Mammalian Evolution." *The American Naturalist* 168.2 (2006): 270-280.

Goswami, A. "Cranial modularity and sequence heterochrony in mammals." *Evolution & Development* 9.3 (2007): 290-298.

Goswami, A., and P.D. Polly. "The Influence of Modularity on Cranial Morphological Disparity in Carnivora and Primates (Mammalia)." *PLoS One* 5.3 (2010): e9517.

Goswami, A., Smaers, J.B., Soligo, C., and P.D. Polly. "The macroevolutionary consequences of phenotypic integration: from development to deep time." *Philosophical Transactions of the Royal Society B* 369 (2014): 20130254.

Haber, A. "unifyVD.R." http://life.bio.sunysb.edu/morph/morphmet/unifyVD.R (2011).

Hautier, L., Michaux, J., Marivaux, L., and M. Vianey-Liaud. "Evolution of the zygomasseteric construction in Rodentia, as revealed by a geometric morphometric analysis of the mandible of Graphiurus (Rodentia, Gliridae)." *Zoological Journal of the Linnean Society* 154 (2008): (807-821).

Houle, A. "The origin of platyrrhines: An evaluation of the antarctic scenario and the floating island model." *American Journal of Physical Anthropology* 109 (1999): 541–559.

Huchon, D. and Douzery E.J.P. "From the Old World to the New World: A Molecular Chronicle of the Phylogeny and Biogeography of Hystricognath Rodents." *Molecular Phylogenetics and Evolution* 20.2 (2001): 238-251.

Hussain, S. T., de Bruijn, H., and Leinders, J. M. "Middle Eocene rodents from the Kala Chitta Range (Pujab, Pakistan) (III)". *Proceedings of the Koninklijke Nederlandse Akademie van Wetenschappen: Series B* 81 (1978): 101–112.

Jones, K.E., Bielby, J., Cardillo, M., Fritz, S.A., O'Dell, J., Orme, C.D.L., Safi, K., Sechrest, W., Boakes, E.H., Carbone, C., Connolly, C., Cutts, M.J., Foster, J.K., Grenyer, R., Habib, M., Plaster, C.A., Price, S.A., Rigby, E.A., Rist, J., Teacher, A., Bininda-Emonds, O.R.P., Gittleman, J.L., Mace, G.M., and A. Purvis. 2009. "PanTHERIA: a species-level database of life history, ecology, and geography of extant and recently extinct mammals." *Ecology* 90 (2009):2648.

Kimes, P.K., Liu, Y., Hayes, D.N. and J.S. Marron. "Statistical Significance for Hierarchical Clustering." *Biometrics* DOI: 10.1111/biom.12647 (2017).

Klingenberg, C.P. "Studying Morphological Integration and Modularity at Multiple Levels: Concepts and Analysis." *Philosophical Transactions of the Royal Society B: Biological Sciences* 369 (2014): 20130249.

Lavocat, R. "La syste´matique des rongeurs hystricomorphes et la de´rive des continents." *Comptes Rendus de l'Académie des Sciences Series D* 269 (1969): 1496– 1497.

Liu, Z., Pagani, M., Zinniker, D., DeConto, R., Huber, M., Brinkhuis, H., Shah, S.R., Leckie, R.M., and A. Pearson. "Global Cooling During the Eocene-Oligocene Climate Transition." *Science* 323 (2009): 1187-1190.

Maestri, R., Patterson, B.D., Fornel, R., and T. Freitas. "Diet, bite force, and skull morphology in the generalist rodent morphotype." *Journal of Evolutionary Biology* 29 (2016): 2191-2204.

Mares, M. A., and R.A. Ojeda. (1982). "Patterns of diversity and adaptation in South American hystricognath rodents." *Mammalian biology in South America* (1982): Eds. M. A. Mares & H. H. Genoways (pp. 393–432). Linesville: Special Publication Pymatuning Laboratory of Ecology.

Marroig, G., Shirai, L.T., Porto, A., Oliveira, F.B., and V. Conto. "The Evolution of Modularity in the Mammalian Skull II: Evolutionary Consequences." *Evolutionary Biology* 36.1 (2009): 136-148.

Martin, T. "African origin of caviomorph rodents is indicated by incisor enamel microstructure." *Paleobiology* 20 (1994): 5–13.

Millien, V. "The Largest Amongst the Smallest: the Body Mass of the Giant Rodent *Josephoartigasia monesi.*" *Proceedings of the Royal Society B: Biological Sciences* 275 (2008): 1953-1955.

Millien, V., and H. Bovy. "When Teeth and Bones Disagree: Body Mass Estimation of a Giant Extinct Rodent." *Journal of Mammalogy* 91.1(2010): 11-18.

Myers, P. "Chinchillidae: chinchillas and viscachas." *Animal Diversity Web*. University of Michigan. Animaldiversity.org.

Myers, P. "Chinchillidae: chinchillas and viscachas." *Animal Diversity Web*. University of Michigan. Animaldiversity.org.

Myers, P. "Dasyproctidae: acuchis and agoutis." *Animal Diversity Web*. University of Michigan. Animaldiversity.org.

Myers, P. "Dinomyidae: pacarana." *Animal Diversity Web.* University of Michigan. Animaldiversity.org.

Myers, P. "Echimyidae: spiny rats." *Animal Diversity Web.* University of Michigan. Animaldiversity.org.

Myers, P. "Octodontidae: degus, rock rats, and viscacha rats." *Animal Diversity Web.* University of Michigan. Animaldiversity.org.

Nowak, R. M. *Walker's mammals of the world, 5th ed.* (1991). Baltimore: Johns Hopkins University Press.

Olsen, A.M. and M.W. Westneat. "StereoMorph: an R package for the collection of 3D landmarks and curves using a stereo camera set-up." *Methods in Ecology and Evolution* 6.3 (2015): 351-356.

Olson, E.C., and R.L. Miller." Morphological Integration." *The University of Chicago Press,* Chicago (1958).

Opazo, J.C. "A molecular timescale for caviomorph rodents (Mammalia, Hystricognathi)." *Molecular Phylogenetics and Evolution* 37 (2005): 932-937.

Patton, J. L., Pardiñas, U. F. J., and G. D'Elía. *Mammals of South America, Vol. 2, Rodents* (2015). Chicago: The University of Chicago Press.

Pigliucci, M., and K. Preston. "Phenotypic Integration." *Oxford University Press*, Oxford (2004).

Porto, A., Oliveira, F.B., Shirai, L.T., Conto, V., and G. Marroig. "The Evolution of Modularity in the Mammalian Skull I: Morphological Integration Patterns and Magnitudes." *Evolutionary Biology* 36.1 (2009): 118-135.

Poux, C., Chevret, P., Huchon, D., de Jong, W.W. and E.J.P. Douzery. "Arrival and Diversification of Caviomorph Rodents and Platyrrhine Primates in South America." *Systematic Biology* 55.2 (2006): 228-244.

R Core Team. "R: A language and environment for statistical computing." *R Foundation for Statistical Computing,* Vienna, Austria. R-project.org, 2015.

Red List. "The IUCN List of Threatened Species." *International Union for Conservation of Nature and Natural Resources.* Cambridge, United Kingdom. Iucnredlist.org.

Rinderknecht, A., and R.E. Blanco. "The largest fossil rodent." *Proceedings of the Royal Society B: Biological Sciences* 275.1637 (2008): 923-928.

Rohlf, F. J. " tpsDig." Department of Ecology and Evolution, State University of New York, Stony Brook (2010).

Rohlf, F. J. "Morphometrics." *Annual Review of Ecology, Evolution and Systematics* 21 (1990): 299-316.

Rohlf F.J. and L.F. Marcus. "A revolution in morphometrics." *Trends in Ecology & Evolution* 8 (1993): 129–132.

Sanchez-Villagra, M.R., Aguilera, O., and I. Horovitz. "The Anatomy of the World's Largest Extinct Rodent." *Science* 301.5640 (2003): 1708-1710.

Shimodaira, H. "An Approximately Unbiased Test of Phylogenetic Tree Selection." *Systematic Biology* 51.3 (2002): 492-508.

Shimodaira, H. "Approximately unbiased tests of regions using multistep-multiscale bootstrap resampling." *The Annals of Statistics* 32.6 (2004): 2616-2641.

Suzuki, R. and H. Shimodaira. "Pvclust: an R package for assessing the uncertainty in hierarchical clustering." *Bioinformatics* 22.12 (2006): 1540-1542.

Vermeij, G.J. "Adaptation, versatility, and evolution." *Systematic Zoology* 22 (1973): 466-477.

Vizcaino, S.F., Kay, R.F., and M.S. Bargo, eds. "Early Miocene Paleobiology in Patagonia: High-Latitude Paleocommunities of the Santa Cruz Formation." *Cambridge University Press*, Cambridge (2012).

Webster, M. and H.D. Sheets. "A Practical Introduction to Landmark-Based Geometric Morphometrics." *The Paleontological Society Papers* 16 (2010): 163-188.

Wyss, A. R., Flynn, J. J., Norell, M. A., Swisher, C. C. III, Charrier, R., Novacek, M. J., and McKenna, M. C. "South America's earliest rodent and recognition of a new interval of mammalian evolution." *Nature* 365 (1993): 434–437.

Zelditch, M.L., Swiderski, D.L. and H.D. Sheets. "Geometric Morphometrics for Biologists: A Primer (2nd Edition)." *Elsevier Inc.*, London (2012).